

Semimetallic Antiferromagnetism in the Half-Heusler Structure: CuMnSb

T. Jeong,¹ Ruben Weht,² and W. E. Pickett¹

¹*Department of Physics, University of California, Davis CA 95616*

²*Departamento de Física, CNEA, Avda. General Paz y Constituyentes, 1650 - San Martín, Argentina*

(Dated: August 30, 2018)

The half-Heusler compound CuMnSb, the first antiferromagnet (AFM) in the Mn-based class of Heuslers and half-Heuslers that contains several conventional and half metallic ferromagnets, shows a peculiar stability of its magnetic order in high magnetic fields. Density functional based studies reveal an unusual nature of its unstable (and therefore unseen) paramagnetic state, which for one electron less (CuMnSn, for example) would be a zero gap semiconductor (accidentally so) between two sets of very narrow, topologically separate bands of Mn 3d character. The extremely flat Mn 3d bands result from the environment: Mn has four tetrahedrally coordinated Cu atoms whose 3d states lie well below the Fermi level, and the other four tetrahedrally coordinated sites are empty, leaving chemically isolated Mn 3d states. The AFM phase can be pictured heuristically as a self-doped $\text{Cu}^{1+}\text{Mn}^{2+}\text{Sb}^{3-}$ compensated semimetal with heavy mass electrons and light mass holes, with magnetic coupling proceeding through Kondo and/or antiKondo coupling separately through the two carrier types. The ratio of the linear specific heat coefficient and the calculated Fermi level density of states indicates a large mass enhancement $m^*/m \sim 5$, or larger if a correlated band structure is taken as the reference.

PACS numbers: 71.28.+d, 71.20.Be, 71.18.+y

I. INTRODUCTION

The study of unusual magnetic materials has increased dramatically in the past decade, due to new phenomena such as colossal magnetoresistance, half-metallic ferromagnetism, spin gaps and novel heavy fermion behavior, to name a few. The Heusler (AT_2X type) and half Heusler (ATX type, T = transition metal, X = metal or metalloid) structures have produced a number of unusually interesting compounds. For example, ferromagnetic (FM) PtMnSb was discovered¹ to display the largest known magneto-optic Kerr effect at room temperature (at photon energy $\hbar\omega = 1.75$ eV). A number of them have been proposed as half metallic ferromagnets, and NiMnSb (with one more electron than CuMnSb) is one of the most widely accepted examples of half metallic ferromagnetism.

We address here the half-Heusler compound CuMnSb, which has its own peculiarities. In a class of intermetallic magnets where ferromagnetism (FM) can occur as high as 1000 K, CuMnSb develops antiferromagnetism (AFM) at the relatively low temperature, with reports of $T_N = 55$ K from Endo,² 62 K from Helmholdt *et al.*,³ and 50 K from Boeuf.⁴ A large value of the ordered Mn moment $m = 3.9\text{-}4.0 \mu_B$ has been obtained from neutron scattering measurements.^{3,5} This moment suggests that a “monovalent Mn” may provide a good picture, with $d_{\uparrow}^5, d_{\downarrow}^1$ high spin configuration. The Curie-Weiss moment is large, reported variously as $5.4 \mu_B$ [2], $6.3 \mu_B$ [4] and $7.2 \mu_B$, [6] the latter two of which would be more consistent with a “divalent Mn” $d_{\uparrow}^5, d_{\downarrow}^0$ configuration. The Curie-Weiss $\theta_{CW} = -160$ K suggests large AFM interactions between the Mn moments², consistent with the AFM ordering.

CuMnSb is metallic, but experimentally much less so

than the FM compounds in its class. Its Drude plasma energy was reported⁷ as $\hbar\Omega_p = 1.6$ eV compared to 2.6-6 eV for the FM Heusler compounds, suggesting a much smaller density of states and/or Fermi velocity, and an interband absorption peak was reported at 0.8 eV.⁸ For a metal, the square Ω_p^2 is proportional to $N(E_F)v_F^2$ (often interpreted as an effective carrier density to mass ratio $(n/m)_{eff}$), and this square is a factor or 3-15 lower than its FM counterparts.

The resistivity of CuMnSb shows a fairly rapid drop below T_N , with the samples of Schreiner and Brandão⁹ dropping from around $170 \mu\Omega \text{ cm}$ above T_N to $50 \mu\Omega \text{ cm}$ at low temperature. More recent work⁴ has lowered these numbers somewhat: $120 \mu\Omega \text{ cm}$ above T_N to $45 \mu\Omega \text{ cm}$ at low temperature. Such resistivity drops at magnetic ordering transitions are common and reflect spin scattering that gets frozen out in the ordered phase. In contradiction to this inference, and quite unusual for magnetic compounds, CuMnSb shows little magnetoresistance.^{4,6} The still large residual resistivity ($\approx 45 \mu\Omega \text{ cm}$)¹⁰ in the best samples suggests some intersite disorder or non-stoichiometry (the empty site makes half Heuslers susceptible to such defects). Our work indicates this compound to be a semimetal, however, so this residual resistivity alternatively may reflect primarily a low carrier density for a metal. In both AFM CuMnSb and several FM half Heusler compounds, it has reported that the resistivity is not T^2 at low temperature,¹⁰ however Boeuf⁴ obtains essentially a T^2 behavior.

Possibly related to some of these features is the fact that CuMnSb displays a curious stability of its magnetic order under applied magnetic fields. The Néel temperature is invariant for fields up to 14 T. Whereas many AFMs display metamagnetic transitions in a field, the induced moment at 5 K and $H = 12$ T is only $0.25 \mu_B$,

again reflecting its imperviousness to applied fields. In a more recent work Doerr et al.¹¹ have seen no changes of the antiferromagnetic characteristics up to 50 T.

The remaining evidence about the electronic state of CuMnSb is from heat capacity (C_V) data.^{4,6} The linear specific heat coefficient $\gamma = 17$ mJ/mol K² corresponds to a quasiparticle density of states $N^*(E_F) = 7.2$ states/eV per formula unit. The T^3 coefficient of C_V was reported to be two orders of magnitude larger than the anticipated lattice contribution, which by itself would suggest it is dominated by soft magnetic fluctuations. Half-Heusler antimonides have recently attracted attention due to their large thermopower and other promising thermoelectric properties,¹² but the Seebeck coefficient of CuMnSb has not been reported.

Although there has been almost no electronic structure study of CuMnSb, many other Heusler and half Heusler compounds have been studied rather thoroughly. A recent analysis of trends in the electronic structure and magnetization of Heusler compounds was presented by Galanakis, Dederichs, and Papanikolaou,¹³ which references much of the earlier work. A recent review concentrating on spintronics applications has been provided by Palmstrom.¹⁴ An extensive set of calculations for many half Heusler compounds has been presented by Nanda and Dasgupta.¹⁵ None of these address Cu-containing compounds, however.

In this paper we lay the foundations for an understanding of the electronic properties and magnetism of CuMnSb by reporting local spin density results for the electronic and magnetic structures, and the equation of state, for unpolarized, ferromagnetic, and antiferromagnetic alignment of the Mn spins. The results, such as the AFM ordering and the low density of states at the Fermi level $N(E_F)$, are in reasonable agreement with experimental data, so it appears that LSDA is accurate for CuMnSb as it is in most other intermetallic $3d$ compounds. The resulting band structure in the AFM phase is rather unusual, being that of a compensated semimetal with normal mass hole bands but heavy mass electron bands. Possible correlation effects are investigated using the correlated band theory (LDA+U) method.

II. STRUCTURE AND METHOD OF CALCULATION

The half Heusler structure is based on the Heusler structural class AT_2X of numerous intermetallic compounds, with space group $Fm\bar{3}m$ (#225) whose point group contains all 48 cubic operations. This structure type can be pictured in terms of an underlying bcc arrangement of atomic sites with lattice constant $a/2$, with atom A at $(0,0,0)$, X at $(\frac{1}{2}, \frac{1}{2}, \frac{1}{2})a$, and T at $(\frac{1}{4}, \frac{1}{4}, \frac{1}{4})a$ and $(\frac{3}{4}, \frac{3}{4}, \frac{3}{4})a$. Thus the T and X sites lie on the corner sites of the bcc lattice (alternating), while the A sites comprise the body center sites. In the half Heusler structure, one of the T sites is unoccupied. The CuMnSb therefore can

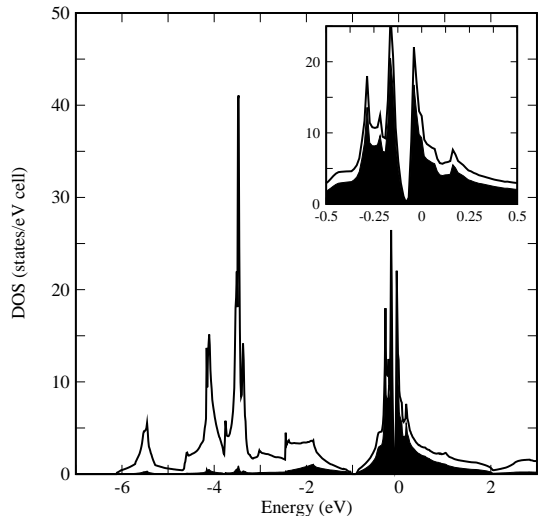


FIG. 1: Density of states of nonmagnetic CuMnSb, with the Mn $3d$ contribution shaded. The inset shows the anomalous accidental “zero gap” that occurs slightly below E_F .

be viewed as “MnCu₂Sb” with the Cu site at $(\frac{1}{2}, \frac{1}{2}, \frac{1}{2})a$ unoccupied.

There are alternative views of the structure. For example, in AT_2X , the A and X sites form a rocksalt lattice and the T atoms fill the tetrahedral sites of this lattice. Alternatively, in half Heusler ATX , A and T form a zincblende lattice and half of the interstices (those neighboring T) are filled with X atoms. An alternative view of last choice is the viewpoint of a zincblende lattice formed of T and X atoms, with A placed at the interstitial site nearest T. We will study whether any of this viewpoints is preferable to the others.

The half Heusler structure has space group $F\bar{4}3m$ (#216) with the tetrahedral point group. The crystal structure⁵ is fcc, lattice constant $a = 6.088$ Å, with Mn (A) at $(0,0,0)$, Cu (T) at $(\frac{1}{4}, \frac{1}{4}, \frac{1}{4})$ and Sb (X) at $(\frac{1}{2}, \frac{1}{2}, \frac{1}{2})$. The symmetry of all the sites is $\bar{4}3m$. It will become significant that in this structure the magnetic atom Mn is coordinated tetrahedrally by four Cu atoms at $(\sqrt{3}/4)a = 2.64$ Å, with the other four nearest sites being vacant. Mn is second-neighbored by six Sb atoms at a distance of $a/2 = 3.04$ Å. The Mn-Cu distance is almost identical to the sum of their atomic radii (1.35 Å and 1.28 Å, respectively), while the Mn-Sb distance is 3% greater than the sum of their radii (1.35 Å and 1.59 Å, respectively). The AFM structure consists of alternating (111) planes of Mn atoms with aligned spins. The Mn-Mn nearest neighbor distance of 4.31 Å assures that direct Mn-Mn exchange is not a dominant factor in the magnetic ordering.

Two types of band structure methods have been used. The full-potential nonorthogonal local-orbital minimum-basis scheme (FPLO)^{16,17} was used for scalar relativistic calculations in the local density approximation (LDA) for the exchange-correlation energy¹⁸. Cu $3s, 3p, 4s, 4p, 3d$,

Mn $3s$, $3p$, $4s$, $4p$, $3d$, and Sb $4s$, $4p$, $5s$, $5p$, $4d$ states were included as valence states. All lower states were treated as core states. We included the relatively extended semi-core $3s$, $3p$ states of Cu and Mn, and $4s$, $4p$ semicore of Sb as band states because of the considerable overlap of these states on nearest neighbors. This overlap would be otherwise neglected in the FPLO scheme. The spatial extension of the basis orbitals, controlled by a confining potential $(r/r_0)^4$, was optimized to minimize the total energy. The self-consistent potentials were calculated on a $12 \times 12 \times 12$ k mesh in the Brillouin zone, which corresponds to 116 k points in the irreducible zone.

For the magnetic calculations the full-potential linearized augmented-plane-wave (FLAPW) method as implemented in the Wien2k code¹⁹ was used. The s , p , and d states were treated using the APW+lo scheme²⁰, while the standard LAPW expansion was used for higher l 's. The basis size was determined by $R_{mt}K_{max} = 7.0$. The space group of the AFM structure is $R3m$ (#160). The results we present result from use of the Perdew-Burke-Ernzerhof generalized gradient approximation form²¹ of exchange-correlation functional, but for the bands and density of states the results are similar to those from the local density approximation.

III. RESULTS OF ELECTRONIC STRUCTURE CALCULATIONS

A. Paramagnetic phase

The (unstable) paramagnetic electronic structure of CuMnSb is unusual. The density of states (DOS), shown in Fig. 1, exhibits a narrow peak around the Fermi level E_F , with an extremely narrow valley slightly below E_F . The five $3d$ bands that in metallic Mn are spread over ~ 5 eV are here confined to a 1 eV region centered on E_F . The split peak is the result of a gap between the disjoint “valence” bands and “conduction” bands, but the gap is indirect and accidentally zero. CuMnSb, with an odd number of valence electrons in the primitive cell, cannot be a nonmagnetic insulator, and the occupied states include one electron in what we are referring to as the conduction bands (those above the tiny gap). The upper valence and lower conduction bands show a *direct* gap of ~ 0.1 eV around the zone edge L, W, and U points. On either side of the gap the bands are flat over most of the surface of the Brillouin zone, and analysis shows that Mn t_{2g} character dominates the bands on both sides of the gap (especially above).

The Heusler and half Heusler structures tend to give rise to such gaps, which is the origin of the various occurrences of half metallic ferromagnetism in this structure. One should take the point of view that CuMnSb contains only one transition metal atom, since the Cu $3d$ ¹⁰ shell is completely filled and thus inert. Therefore the Cu $3d$ states are not involved in a double-peaked complex of narrow bands at E_F . Ironically, we find that the presence

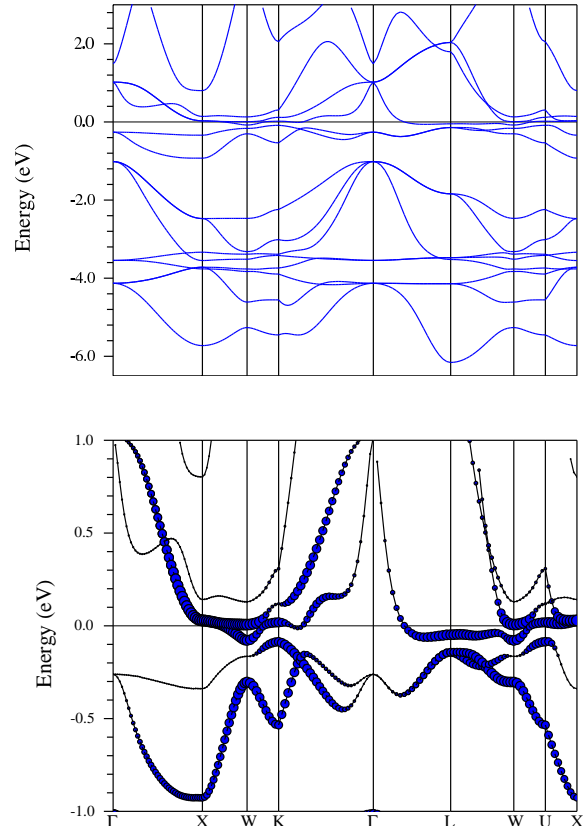


FIG. 2: Top panel: nonmagnetic bands of CuMnSb. Notice that the two bands in the -1 eV to E_F region are disjoint from not only the lower bands, but also the near-lying bands above that have the same Mn $3d$ character. The indirect gap from K to W is accidentally almost zero. Bottom panel: blowup of the bands very near the Fermi level emphasizing the bands with Mn t_{2g} character with larger symbols. Of these five bands, the ones appearing here as thin lines have e_g character.

of Cu in the compound is the key to the peaked Mn $3d$ DOS and possibly to the peculiarity of the magnetism. The Mn atom sits at the center of a minicube in which it is coordinated tetrahedrally by four Cu atoms, and also tetrahedrally by four unoccupied sites in the half Heusler lattice. Hence the Mn $3d$ states have only the p states of the second neighbor Sb atoms (along the cubic axes) and some weak Cu $4s$ character to hybridize with and hence to broaden. This coupling is weak, as reflected in the narrow Mn DOS. To establish the effect of Cu quantitatively for states around the Fermi level, we also carried out a calculation of O^{+1}MnSb , which denotes CuMnSb with the Cu atom removed but leaving its $4s$ electron (which is simply added to the system). The change is very small near E_F , the one effect being that the three-fold level above E_F at the zone center is shifted upward by 0.6 eV by the presence of Cu.

Whether or not the paramagnetic phase has a Stoner instability, it is clear from the huge DOS peaks that a

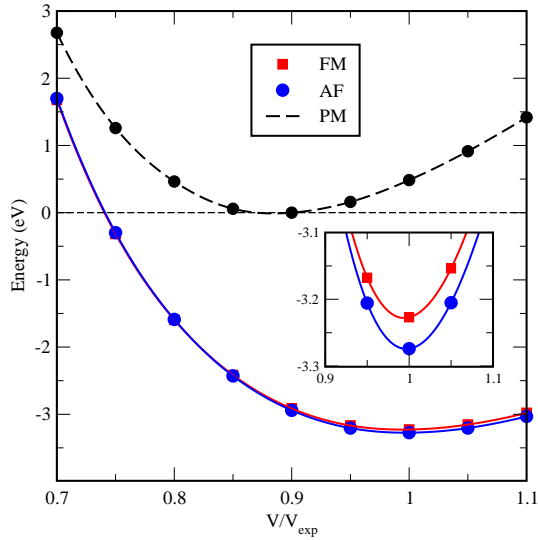


FIG. 3: Calculated equation of state for nonmagnetic (upper curve) and magnetic (lower curves) CuMnSb. On this scale the FM and AFM differences cannot be distinguished. Note the extremely large magnitude of the energy gain from magnetism, and the very large “magnetic expansion” corresponding to almost 4% in the lattice constant.

FM state with finite moment is likely to be energetically favorable to the paramagnetic state. The calculated Fermi level DOS is $N(E_F) = 11.68$ states/eV per formula unit, which corresponds to a linear specific heat coefficient (without any many body enhancement) of 27.5 mJ/mol-K². Assuming the usual value of Stoner interaction parameter $I_{Mn} \approx 0.75$ eV leads to $N(E_F)I \sim 9$, reflecting a very strong Stoner instability (which occurs anytime $N(E_F)I \geq 1$).

B. Ferromagnetic alignment of Mn spins

Calculation shows that either FM or AFM order lowers the energy by more than 3 eV/Mn compared to a nonmagnetic configuration, reflecting the energy gain simply from local moment formation. In addition, there is an energy difference arising from the type of spin alignment. In Fig. 3 the equation of state is pictured for the paramagnetic, FM, and AFM phases. The energy difference between FM and AFM phases is about 50 meV, a factor of 60 smaller than the energy gain from moment formation. Hence the Mn moment will be very robust in this compound, independent of degree or type of order. Also noteworthy is the large difference in volumes, the paramagnetic equilibrium being about 12% smaller in volume (4% smaller lattice constant) than the magnetic phases.

Before moving on to discuss the more stable AFM electronic structure, we analyze briefly the FM results. The exchange splitting of the Mn 3d states is 3.5 eV, thus the FM bands look nothing like rigidly shifted replicas of the paramagnetic bands, as is evident from the DOS pic-

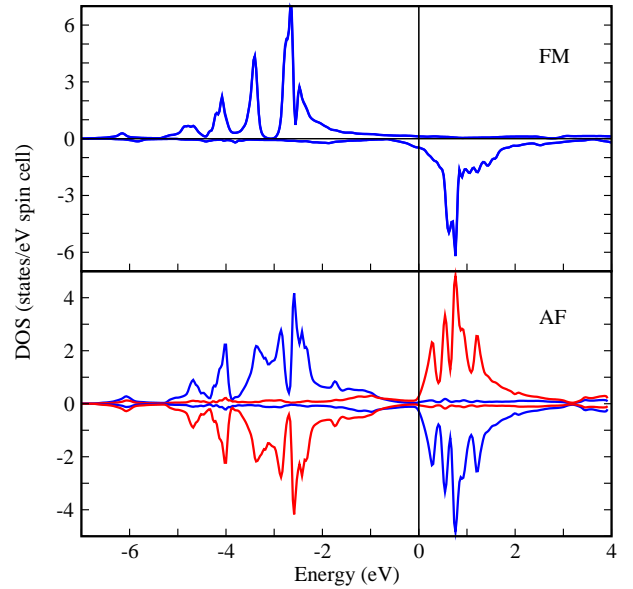


FIG. 4: Comparison of the Mn partial densities of states for the magnetic (FM and AFM) configurations. For FM alignment there is some occupation of the minority bands that is evident in the figure. Though less obvious, there is also minority occupation in the AFM, and the moment is $4 \mu_B$.

tured in Fig. 4. For the unpolarized bands up and down bands are identical and both are about half-filled; after spin polarization, the majority are filled and the minority are nearly empty. The large exchange splitting is characteristic of the large moment, $3.9 \mu_B$ in the Mn sphere, $0.1 \mu_B$ from the Cu sphere, and $0.4 \mu_B$ in the interstitial, for a total of $4.4 \mu_B$ per formula unit. The interstitial contribution is perhaps mostly from Mn tails, since the Mn majority states are clearly entirely filled (Fig. 4) but there is some small filling of the Mn minority 3d states that will reduce the moment somewhat, *i.e.* $5 (\uparrow) - 0.6 (\downarrow) = 4.4 \mu_B$.

Once the moment is formed, the majority Mn 3d bands overlap the Cu 3d bands in energy and mix strongly, and together form two nearly dispersionless complexes of bands along Γ -A at -3.4 eV and -2.75 eV. This repulsive hybridization with the closed 3d shell of Cu should contribute to the large lattice expansion noted above, which is larger than that due to the conventional volume expansion due to moment formation. The minority Mn 3d states hybridize only with Sb 5p or Cu 4s, and form a narrow set of bands 0.8 eV above E_F that is only 0.4 eV wide (with some tailing). The resulting Fermi level DOS is quite low, $N(E_F) = 0.505$ (up) + 0.845 (down) = 1.35 states/eV per formula unit. While this FM alignment is metastable, the EOS calculations show that AFM alignment is more stable, in agreement with experiment. Between the exchange split Mn 3d states lie bands with 2-3 eV dispersion that have primarily Sb 5p character.

C. Antiferromagnetic alignment of Mn spins

We obtain an AFM state for CuMnSb whose Mn $3d$ density of states is shown in Fig. 4. The magnetic moment lies almost entirely on the Mn atom, which is essentially a fully occupied majority and some minority occupation, with moment $m = 3.9 \mu_B$ within the Mn sphere of radius 2.2 bohr, in excellent agreement with the measured ordered moment.^{3,5} The Mn exchange splitting is 3.5 eV, the same as for the FM case and again consistent with the large moment.

Fig. 4 reflects also a very low density of states at E_F , whose value is $N(E_F) = 1.38$ states/eV per formula unit. As in the paramagnetic phase, the valence and conduction bands are disjoint, as can be seen in Fig. 5. There are two small, and one larger, Fermi surface hole cylinders along the Γ -A $(0, 0, k_z)$ line in this figure, which corresponds to one Γ -L $\langle 111 \rangle$ direction in the original fcc zone. These holes are compensated by electron pockets at the X point of the fcc zone.

D. Possible correlation corrections: LDA+U

It is common for the local spin density approximation to work very well for transition metal intermetallics and in compounds with pnictides, and it has been used extensively in the Heusler and half-Heusler classes. Given the relative chemical isolation of the Mn moment in CuMnSb, however, one may wonder if there are residual correlations effects that should be accounted for, such as with the LDA+U method.²⁵ LDA+U is known to do a good job of modeling the band equivalent of the Mott insulator in several systems, mostly oxides. CuMnSb is a metal, and in fact the calculated LSDA DOS seems to be at least qualitatively reasonable compared to the quasiparticle DOS obtained from the linear specific heat coefficient. Still, it is important to know if correlation corrections could change the results appreciably.

We have applied the LDA+U functional as adapted to the linearized augmented plane wave method by Shick *et al.*²⁶ and implemented in the Wien2k code to investigate this question. The LDA+U method requires the values of the Mn $3d$ Coulomb repulsion U and exchange J constants. Because we use the “fully-localized limit” form²⁷ of functional, we make the common replacement $U \rightarrow U_{eff} \equiv U - J$, and have tried the values $U = 2.5, 5.0, \text{ and } 7.5$ eV. The resulting total and Mn-projected DOS are shown in Fig. 6. The occupied and unoccupied Mn $3d$ states behave as expected, each moving away from the Fermi level as U is increased. Except for reduction of hybridization due to this shift of $3d$ states, the bands are changed little. In particular, the band overlap describing a compensated semimetal remains, however it is increased by 0.2 eV. The calculated values of $N(E_F)$ for $U = 0, 2.5, 5.0, \text{ and } 7.5$ eV are 1.38, 0.76, 0.66, and 0.66 states/eV cell (both spins), respectively. Thus the effect of including U is to *reduce* the *band* mass by as much as

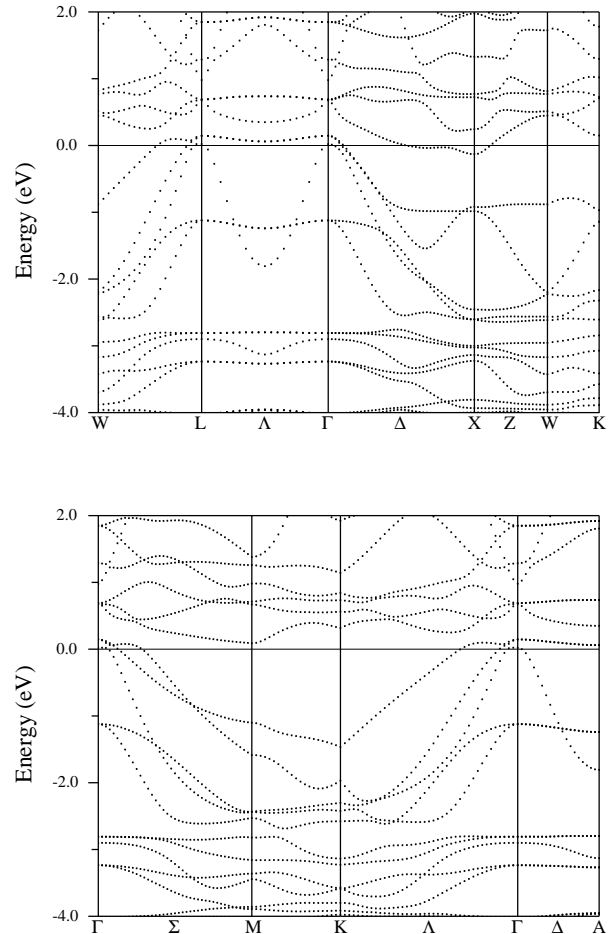


FIG. 5: Bands of antiferromagnetic CuMnSb, plotted along lines in both the underlying fcc symmetry (top) and in the hexagonal AFM symmetry (bottom). The Γ -L direction shown is along the hexagonal axis of the AFM cell. As for the paramagnetic phase, the bands (primarily) below $E_F=0$ (valence) are disjoint from those above (conduction), but each overlap E_F by 0.1 eV. The exchange split Mn $3d$ bands lie around -3 eV and +0.5 eV.

50%, due to the reduction of the minority Mn $3d$ character in the conduction bands. The corresponding values of the Mn moment (inside the muffin-tin sphere) are 3.87, 4.20, 4.40, 4.52 μ_B respectively.

The band structure for $U = 5$ eV (which is probably an upper limit for the value of U for Mn in an intermetallic compound) is shown in Fig. 7. The increased band overlap, relative to $U=0$, results in larger Fermi surfaces for both electrons and holes. There is a single electron ellipsoid (at the point that would be X in the cubic Brillouin zone), while there are three closed hole surfaces around both the Γ and A points of the hexagonal Brillouin zone.

The separation (disjointness) between the conduction and valence bands becomes clearer when $U > 0$ is included (Fig. 7), which reflects some sort of ‘bonding -

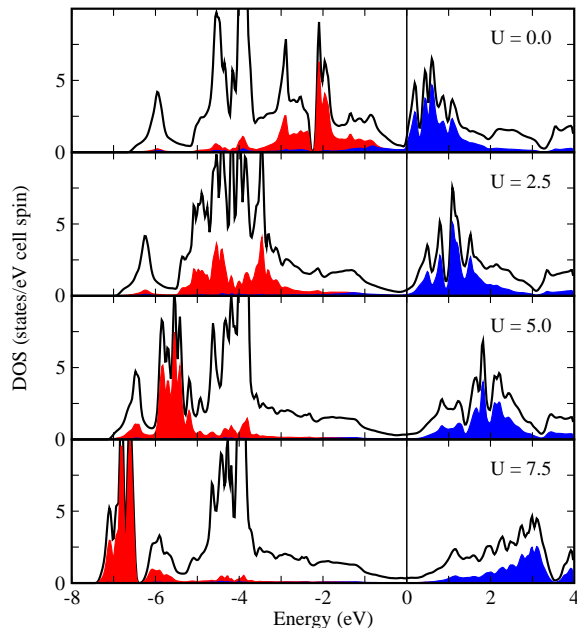


FIG. 6: (color online) Total and Mn 3*d*-projected (filled-in regions) density of states of CuMnSb, using the LDA+*U* method with $U = 0$ (LDA), 2.5, 5.0, and 7.5 eV (top to bottom). The only noteworthy change is the lowering of occupied, and raising of unoccupied, Mn 3*d* states. The small DOS around the Fermi level remains.

antibonding' separation that is not very clear in terms of interaction of atomic orbitals. One might then be concerned about the 'band gap problem' in the local density approximation, for which a gap separating bands of distinctly different character is usually underestimated. One approximate remedy for this problem is the GW approximation, in which a nonlocal dynamically screened exchange interaction is included.²⁸ The projected density of states however shows no clear distinction between the characters of the *s* – *p* bands below and above the gap, so the self-energy correction is not likely to be large. Since the band structure is that of a heavily doped self-compensated semiconductor (whether with $U = 0$ or $U = 5$ eV), any correction will have some effect on the carrier density and on the value of $N(E_F)$.

IV. DISCUSSION AND SUMMARY

In this local-density based study of the electronic and magnetic structure of the half-Heusler magnet CuMnSb we have found AFM alignment to be energetically favored, consistent with experiment. The moments, for which the LSDA value of $4 \mu_B$ is in excellent agreement with the observed ordered moment, are robust independent of relative orientation. The characters of occupied

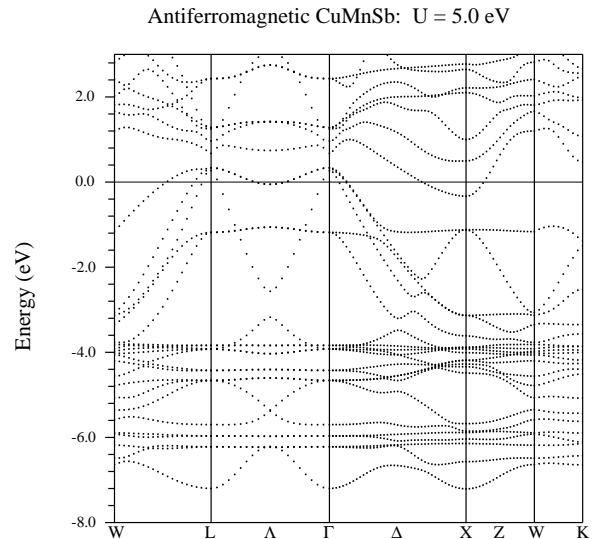


FIG. 7: Bands of CuMnSb using the LDA+*U* method, with $U = 5$ eV. The bands are plotted along the underlying fcc lines (compare to the upper panel of Fig. 5) so both electron and hole pockets are evident. The most noticeable effect of including U is the lifting of minority 3*d* bands to the range 1-3 eV, and almost completely eliminated 3*d* character at the Fermi level.

states indicate that a $\text{Cu}^{1+}\text{Mn}^{2+}\text{Sb}^{3-}$ configuration may be useful starting point for characterizing the electronic structure, although within LSDA there is clearly some minority 3*d* occupation. The electronic structures of all phases are representative of narrow Mn 3*d* bands in the midst of much broader bands consisting of Cu 4*s*, Sb 5*s*5*p*, and, further above, Mn 4*s*, and are consistent with earlier calculation of the density of states.²²

The (LSDA) energy difference of 50 meV/Mn between AFM and FM alignment of spins translates, in a nearest neighbor exchange coupling model, to $J S^2 = 8.3$ meV which with $S = \frac{5}{2}$ gives $J = 1.3$ meV = 15 K. Such a picture of coupling is probably not of quantitative value for CuMnSb, because here interactions between Mn spins will be mediated by a low density of semimetal carriers, leading to coupling with several neighboring shells. There will be two distinct interactions, one through the heavy conduction electrons, another through the light valence band holes. This situation has much in common with EuB_6 , which a recent study²³ has shown to have two such local-moment to itinerant-state interactions, with a different sign of the on-site Kondo coupling for valence and conduction bands.

The calculated LDA value of $N(E_F) = 1.38$ states/eV per formula unit can be compared with the dressed one obtained from the linear specific heat coefficient $N^*(E_F) = 7.2$ states/eV per formula unit to obtain a dynamic thermal mass enhancement $\lambda = m^*/m - 1 \approx 4.2$.

This result is indicative of a large mass enhancement due to spin fluctuations. For $U = 5$ eV, $N(E_F)$ drops to 0.66 states/eV per formula unit and thermal mass enhancement increases to $\lambda \approx 10$.

This nonmagnetic electronic structure is reminiscent of paramagnetic FeSi, in which there is a tiny gap²⁴ of 0.13 eV between flat bands that are of mostly Fe character. In FeSi the Fe moment is very obvious in the Curie-Weiss susceptibility at higher temperature but becomes compensated at low temperature and the ground state is paramagnetic. In CuMnSb the electron count is such that there is one electron above a similar looking gap. The other clear difference is that the Mn atom remains strongly polarized in CuMnSb, while the Fe atom in FeSi loses its magnetism at low temperature.

Our study of the electronic structure of CuMnSb reveals that the Mn 3d states are virtually chemically isolated from the environment, leading to very narrow 3d bands and a strong Stoner instability. In the (observed and predicted) antiferromagnetic state, the system is semimetallic, with rather normal mass Sb 5p hole bands. These bands overlap a single electron band, whose character depends on whether LDA is accurate or if correlations are appreciable. Within LDA, the electron band contains some minority Mn 3d character, while this mixing rapidly disappears if U is appreciable. Comparing the calculated $N(E_F)$ to the specific heat γ indicates a mass enhancement $m^*/m \sim 5$ (LDA) or as much as $m^*/m \sim 11$ ($U \geq 5$ eV). The observed temperature dependence of the transport coefficients show no evidence of heavy

fermion behavior, however.

In the transition metal based Heusler and half-Heusler compounds ferromagnetism is common; CuMnSb is practically the only antiferromagnet. Our calculations indeed predict that AFM has the lower energy, although exploring the spin coupling mechanisms has not been the purpose of this work. The magnetic interactions presumably are mediated separately through the hole and electron bands, indeed it could be the case that the two mechanisms compete, as has been uncovered recently²³ for EuB₆.

The role of the Cu atom is as a spacer and donor of an electron. Cu is nevertheless crucial, since without it MnSb crystallizes in the hexagonal NiAs structure and is ferromagnetic rather than antiferromagnetic. Electronic structure studies of the NiAs-structure phase as well as the possible zincblende phase have been reported previously.²⁹

V. ACKNOWLEDGMENTS

We gratefully acknowledge illuminating discussions with C. Pfleiderer, who also provided a copy of Ref. 4. This work was supported by DOE grant DE-FG02-04ER46111. R.W. is member of CONICET (Consejo Nacional de Investigaciones Científicas y Técnicas, Argentina).

-
- ¹ P. G. van Engen, K. N. J. Buschow, and R. Jongenbreur, *Appl. Phys. Lett.* **42**, 202 (1983).
- ² K. Endo, *J. Phys. Soc. Japan* **29**, 643 (1970); K. Endo, T. Ohoyama, and R. Kimura, *J. Phys. Soc. Japan* **25**, 907 (1968).
- ³ R. B. Helmholtz, R. A. de Groot, F. M. Mueller, P. G. van Engen, and K. H. J. Buschow, *J. Magn. Magn. Mat.* **43**, 249 (1984).
- ⁴ Julien Boeuf, dissertation (2003).
- ⁵ R. H. Forster, G. B. Johnston, and D. A. Wheeler, *J. Phys. Chem. Solids* **29**, 855 (1968).
- ⁶ J. Boeuf, A. Faisst, and C. Pfleiderer, *Acta Phys. Polonica B* **34**, 395 (2003).
- ⁷ M. M. Kirillova, A. A. Makhnev, E. I. Shreder, V. P. Dyakina, and N. B. Gorina, *Phys. Stat. Sol. (b)* **187**, 231 (1995).
- ⁸ J. F. Bobo, P. R. Johnson, M. Kautzky, F. B. Mancoff, E. Tuncel, R. L. White, and B. M. Clemens, *J. Appl. Phys.* **81**, 4164 (1997).
- ⁹ W. H. Schreiner and D. E. Brandao, *Solid State Commun.* **43**, 463 (1982).
- ¹⁰ M. J. Otto, H. Feil, R. A. M. Van Woerden, J. Wijngaard, P. J. Van Der Valk, C. F. Ban Bruggen, and C. Haas, *J. Magn. Magn. Mater.* **70**, 33 (1987).
- ¹¹ M. Doerr, J. Boeuf, C. Pfleiderer, M. Rotter, N. Kozlova, D. Eckert, P. Kersch, K.-H. Müller, and M. Loewenhaupt, *Physica B* **346-347**, 137 (2004).
- ¹² K. Mastronardi, D. Young, C.-C. Wang, P. Khalifah, R. J. Cava, and A. P. Ramirez, *Appl. Phys. Lett.* **74**, 1415 (1999).
- ¹³ I. Galanakis, P. H. Dederichs, and N. Papanikolaou, *Phys. Rev. B* **66**, 174429 (2002).
- ¹⁴ C. Palmstrom, *MRS Bulletin* **28**, 725 (2003).
- ¹⁵ B. R. K. Nanda and I. Dasgupta, *J. Phys.: Condens. Matter* **15**, 7307 (2003).
- ¹⁶ H. Eschrig, *Optimized LCAO Method and the Electronic Structure of Extended Systems* (Springer, Berlin, 1989).
- ¹⁷ K. Koepfner and H. Eschrig, *Phys. Rev. B* **59**, 1743 (1999).
- ¹⁸ J. P. Perdew and Y. Y. Wang, *Phys. Rev. B* **45**, 13244 (1992).
- ¹⁹ P. Blaha, K. Schwarz, G. K. H. Madsen, D. Kvasnicka, and J. Luitz, *An Augmented Plane Wave + Local Orbitals Program for Calculating Crystal Properties*, ISBN **3-9501031-1-2**, (Karlheinz Schwarz, Techn. Universität Wien, Austria, 2001).
- ²⁰ E. Sjöstedt, L. Nordström, and D. J. Singh, *Solid State Commun.* **114**, 15 (2000).
- ²¹ J. P. Perdew, K. Burke, and M. Ernzerhof, *Phys. Rev. Lett.* **77**, 3865 (1996).
- ²² A. Jezierski and A. Szytula, *Acta Physica Polonica A* **97**, 607 (2000).
- ²³ J. Kuneš and W. E. Pickett, *Phys. Rev. B* **69**, 165111 (2004).
- ²⁴ L. F. Mattheis and D. R. Hamann, *Phys. Rev. B* **47**, 13114

- (1993).
- ²⁵ V. I. Anisimov, J. Zaanen, and O. K. Andersen, Phys. Rev. B **44**, 943 (1991).
- ²⁶ A. B. Shick, A. I. Liechtenstein, and W. E. Pickett, Phys. Rev. B **60**, 10763 (1999).
- ²⁷ M. T. Czyzyk and G. A. Sawatzky, Phys. Rev. B **49**, 14211 (1994).
- ²⁸ G. Onida, L. Reining, and A. Rubio, Rev. Mod. Phys. **74**, 601 (2002) provide a recent review.
- ²⁹ A. Continenza, S. Picozzi, W. T. Geng, and A. J. Freeman, Phys. Rev. B **64**, 085204 (2001).